Adsorption of Model Asphalt Functionalities, AC-20, and Oxidized Asphalts on Aggregate Surfaces

CHRISTINE W. CURTIS, DOUGLAS J. CLAPP, YOUNG W. JEON, AND BADRU M. KIGGUNDU

This investigation examined the competitive adsorption behavior of asphalt functionalities for silica and the adsorption behavior of AC-20 and asphalts oxidized to different degrees on real and actual aggregates. The competitive affinity for dry silica of paired combinations of seven model functionalities known to be present in asphalt was determined. The affinity shown by the components in a competitive situation was different from that of the individual components. Competitive adsorption was also performed on moistened silica. The nitrogen base, quinoline, was most sensitive to moisture, whereas the sulfoxide was the least sensitive. In addition, asphalt oxidized to different degrees was adsorbed onto silica, alumina, sandstone, and limestone. On moist and dry silica and alumina, AC-20 was adsorbed more than the oxidized asphalts. On limestone and sandstone, the adsorption of AC-20, oxidized asphalt, and their respective asphaltene fractions was concentration dependent. Most of the adsorption behavior fitted the Langmuir model better than the Freundlich model. Monolayer amounts obtained from the Langmuir isotherms decreased with increased oxidation levels. The nature of the adsorbed asphaltic carbon was examined by controlled atmosphere electron microscopy.

The relative affinities for actual aggregates of individual functionalities known to be present in asphalt (*1–5*) have been investigated using single component adsorption onto actual aggregates (*1*). However, single-component adsorption behavior does not fully predict the competitive adsorptive behavior of asphalt on aggregates in an actual pavement environment, because many different functionalities are present in asphalt and compete for the aggregate surface. It is important to know which functionalities in the complex asphalt mixture have a competitive edge for an aggregate surface.

Asphalt oxidizes as it is exposed to the natural forces of rain, sun, and heat. Oxidation of asphalt results in changes in both its chemical and physical properties, including increased viscosity and increased oxygen functionalities (*3,5*). As asphalt oxidizes, changes in the chemical functionalities present may result in changes in the adsorptive behavior of the asphalt onto the different aggregates and in degradation of pavement performance.

This study investigated the adsorptive behavior of asphalt model functionalities and asphalts oxidized to different degrees onto real and model aggregates. Bicomponent adsorption was performed to determine competitive affinities between asphalt functionalities on both dry and moist silica surfaces. The model functionalities chosen were quinoline, representing nitrogen bases; phenol, phenolics; phenylsulfoxide, sulfoxides; benzoic acid, carboxylic acids; benzophenone, ketones; benzylbenzoate, esters; and pyrene, polynuclear aromatics.

AC-20 and oxidized asphalts, prepared from an AC-20 asphalt, were adsorbed from toluene solutions onto silica, alumina, sandstone, and limestone. Silica and alumina, high surface area model aggregates, were used to evaluate adsorption on a chemically pure substance and to predict the behavior of real aggregates. The other two aggregates, sandstone and limestone, were low surface area aggregates currently being used in Alabama roads. The effect of aggregate surface moisture on asphalt adsorption was examined using silica and alumina containing 5 weight percent water. In addition, the adsorption behavior of asphaltenes, extracted from both AC-20 and the oxidized asphalts, was evaluated on sandstone and limestone.

The nature and character of the asphaltic carbon species that was adsorbed onto dry silica were also examined using controlled atmosphere electron microscopy (CAEM) (*6*). This technique follows the changes in the transmission of the adsorbed asphalt layer while it undergoes reaction with oxygen. The different types of deposits can selectively be removed by oxidizing them at different temperatures until only an inorganic residue remains.

EXPERIMENTAL

Adsorption of Model Asphalt Functionalities

Chemicals Used in Adsorption Studies

The seven compounds selected for adsorption were benzoic acid (99+ percent), quinoline (99+ percent), phenylsulfoxide (97 percent), phenol (99+ percent), benzophenone (99+ percent), benzylbenzoate (99+ percent), and pyrene (99+ percent), all supplied by Aldrich. The solvent used was cyclohexane (99+ percent, spectrophotometric grade, Aldrich). The liquid model compounds and cyclohexane were dried by adding activated 4A molecular sieves, and the solids were dried in a vacuum desiccator. Silica gel (Davison Chemical), properties of which are listed in Table 1, was dried prior to use.

C. W. Curtis, D. J. Clapp, and Y. W. Jeon, Chemical Engineering Department, Auburn University, Auburn, Ala. 36849. B. M. Kiggundu, Concorp International, Ltd., Kampala, Uganda.

TABLE 1 PROPERTIES OF ASPHALTS, ASPHALTENES, AND AGGREGATES

Asphalts Oxidation Time	Properties of Asphalts Viscosity, (poise)	Asphaltenes,%	Oxygen, %	Absorptivity (ml/g cm)
0	2,010±23	22.4	0.44	8,192
1.0	7,050±93	22.7		
2.0	32,300±1,100	25.9		8,733
2.5	57,300±1,400	29.4	0.42	
3.0	126,000±6,900	29.5	0.43	8,985
Asphaltenes Prepared from Asphalts, (poise)				
	2,000		0.78	21,930
	57,000		1.1	
	126,000		1.1	20,950

Aggregate Properties	Silica	Alumina	Sandstone	Limestone
Source	Davison	Alcoa	Selma, AL	Tuscumbia, AL Vulcan Materials
Particle Size, μ	250-500	297-595	177-297	177-297
Pore Size, angstroms	150	175		
Surface Area, m^2/g	294	360	0.68	0.64
Pore Volume, cc/g	1.10	0.346	not detectable	not detectable
Purity, DB wt%	99.8		98% SiO_2 (quartz)	84% $CaCO_3$ 15% SiO_2 (quartz)
Iron Content, % as Hematite and Goethite			0.38	1.29

Procedures

A well-stirred, temperature-controlled (25.0 ± 0.1°C), batch adsorption apparatus was used for model adsorption experiments. Adsorption isotherms were obtained from single components having initial concentrations from 1 to 100 mmol. Each mixture was agitated for 1 hr after introduction of 0.5 g dried silica into a 95-ml solution. Samples were taken by filtering through 0.22 μ Teflon MSI filters and were analyzed by ultraviolet (UV) spectroscopy using a Model 250 Gilford spectrometer. Competitive adsorption was performed by using cyclohexane solutions of pairs of model compounds at 40 mmol. Three grams of dried silica were added to 245 ml of solution. The concentrations of each component were monitored by UV at time intervals of 1, 2, 5, 10, 20, 30, 45, and 60 min. Competitive adsorption was also performed on silica containing 10 ± 0.2 weight percent water that was prepared by placing dry silica in a humidifying chamber containing distilled water.

Analysis of Single and Bicomponent Solutions

Quantitation was based on Beer's Law, $A = \varepsilon bc$, where A, ε, b, and c indicate absorbance, molar absorptivity, cell pathlength (1 cm), and solution concentration, respectively. The UV wavelength used for the individual components was 274 nm for quinoline and benzoic acid; 252 nm, phenylsulfoxide; 271.5 nm, phenol; 250 nm, benzophenone; 247 nm, benzylbenzoate; and 295 nm, pyrene. The UV wavelengths used for the different compound pairs were 252 and 274 nm for quinoline and phenylsulfoxide, respectively; 250/271.5 nm, quinoline/phenol; 274/295 nm, quinoline/benzoic acid and quinoline/benzylbenzoate; 250/274 nm, quinoline/benzophenone;

285/310 nm, quinoline/pyrene; 252/271 nm, phenylsulfoxide/phenol; 258/275 nm, phenylsulfoxide/benzoic acid; and 281/310 nm, benzylbenzoate/pyrene. Individual calibration curves were developed using standard solutions of known concentrations. The calculation of amount adsorbed took into account the changes in solution volume due to periodic sample removal from the flask by employing the following mass balance:

$$\sigma_j = (1/W) \sum_{i=1}^{n} [(V - i\Delta V)(C_{i-1,j} - C_{i,j})]$$

where

σ_j = amount of j-th compound adsorbed per gram silica (mmol/g), for $j = 1$ or 2;
W = silica used (g);
V = solution volume (0.25 l);
Δ = sample volume (0.005 l);
C_o = initial concentration of solution prepared (mmolar);
$C_{i,j}$ = concentration of j-th compound of i-th sample taken (mmolar), for $j = 1$ or 2; and
n = number of sample removal performed.

All data obtained from bisolute adsorption experiments were at least duplicated; however, the data of single-component adsorption isotherms were not. The percent relative errors of the duplicate data of quinoline, phenylsulfoxide, phenol, and benzoic acid ranged from 0.48 to 9.03 percent; the average and standard deviation of the percent relative errors were 3.17 percent and 2.43 percent, respectively. In contrast, benzophenone, benzylbenzoate, and pyrene showed more than 10 percent relative error for the duplicate determinations.

Adsorption of AC-20 and Oxidized Asphalts

Asphalts and Aggregates

AC-20 asphalt, obtained from Hunt Oil in Tuscaloosa, Alabama, was produced from 95 percent West Alabama–Mississippi pipeline crude and 5 percent from Pilon crude. The model and actual aggregates used are given in Table 1. All aggregates were dried at 120°C for at least 2 days until constant weight was achieved. Moist silica and alumina were produced by placing them in a humidifying chamber using distilled water for approximately 15 min. The percent aggregate moisture used was 5.0 ± 0.1 percent.

Asphalt Oxidation

AC-20 asphalt was oxidized to four different viscosities, nominally 7,000, 32,000, 57,000, and 126,000 poise, by placing AC-20 in a vessel containing a sparger and heating to 185°C for up to 3 hr. Compressed air was blown at a rate of 4 l/min to mix the asphalt and facilitate oxidation. After oxidation, all samples were stored in a freezer at −20°C to prevent further oxidation. Asphaltenes were obtained from the oxidized asphalts and AC-20, by extraction with n-pentane. The properties of AC-20, oxidized asphalt, and asphaltenes are given in Table 1.

Adsorption of Asphalts

Continuous adsorption experiments were conducted. Asphalt diluted in dried toluene (spectranalyzed, Fisher) flowed through a bed of aggregate at 25 ± 0.1°C and was pumped through a flow-through cell (0.1 or 1.0 cm) where the absorbance at 375 nm was continuously monitored for 8 hr. From the absorbance readings, the solution concentration and the amount of asphalt adsorbed on the aggregate were calculated. The material balance equation used in the calculations was

$$\sigma W = V(C_{Ao} - C_A)$$

where

σ = amount adsorbed per gram of aggregate (g asphalt/g aggregate);
W = aggregate used (g);
V = volume of asphalt solution used (0.027 l);
C_{Ao} = initial concentration of asphalt solution (g/l);
C_A = equilibrium concentration attained after adsorption (g/l).

One gram of either silica or alumina, 3 g of sandstone or limestone, and 27 ml of solution were used. The initial concentrations of the asphalt and asphaltene solutions were varied over a wide range. All data, plotted as amount adsorbed versus equilibrium concentration, are reported; some exact replicates of equilibrium concentration are given.

FTIR Analysis

Infrared analysis of AC-20 and oxidized asphalts was performed using a Nicolet 5SXC FTIR spectrometer. A cell pathlength of 0.7 mm and solution concentrations of 50 g of asphalt and 40 g of asphaltenes per liter of solution (CCl_4 or CS_2) were used.

CAEM Analysis

Specimens for transmission electron microscopy analysis were prepared by grinding silica coated with adsorbed asphalt to a fine powder and then ultrasonically dispersing the powder in butanol. A drop of suspension was applied to a thin graphite support film mounted on a platinum heater ribbon that was then mounted in the gas reaction cell in an electron transmission microscope. The appearance of the specimens was monitored as the temperature was raised to 750°C in the presence of 2 torr oxygen.

RESULTS AND DISCUSSION

Adsorption of Model Asphalt Functionalities

Adsorption Isotherms of Model Functionalities

Individual adsorption isotherms were obtained for each model functionality to observe its adsorption behavior in the concentration range of 0 to 80 mmol, as shown in Figure 1. For each isotherm, the amount adsorbed per gram silica increased

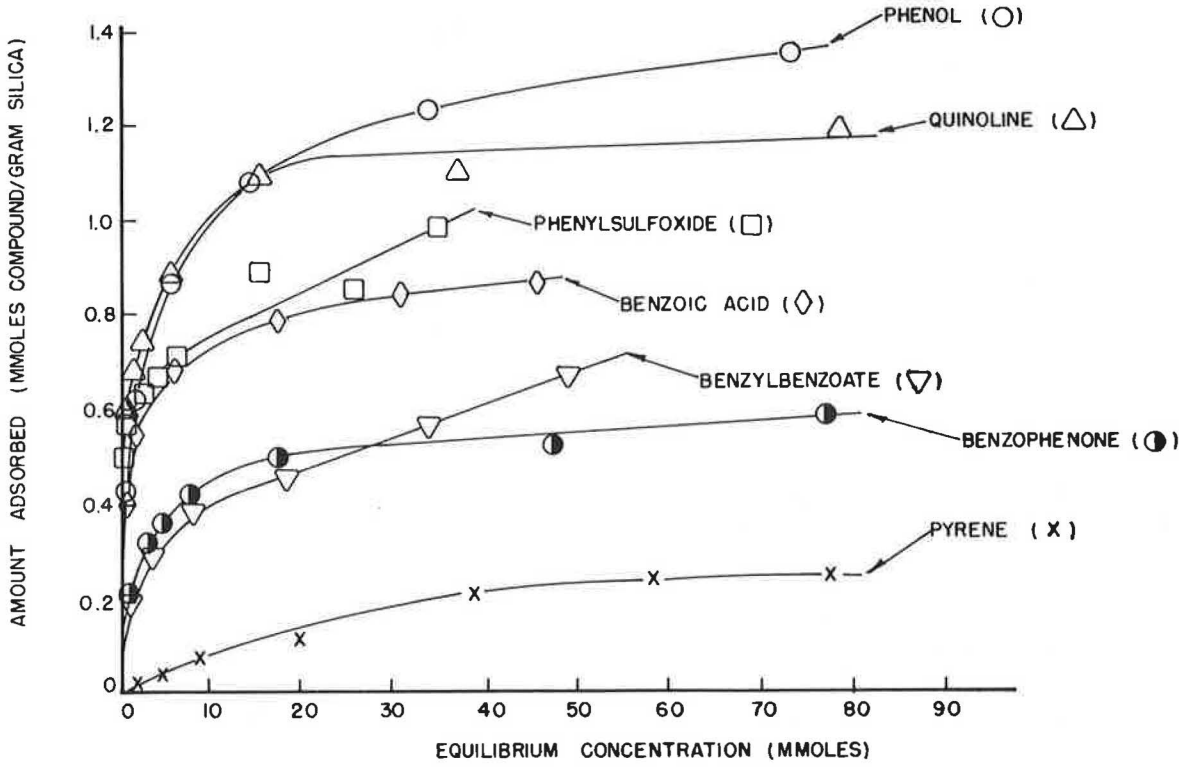

FIGURE 1 Adsorption behavior as a function of equilibrium concentration.

rapidly at low concentrations; as the concentration increased, however, the rate of increase was retarded, forming a concave curve with respect to the concentration. At high concentrations, plateaus were formed except for phenylsulfoxide and benzylbenzoate, which continued to be adsorbed. Their adsorption isotherms could be described only up to ~40 and ~50 mmol, respectively, because of multilayer behavior and limited solubility in cyclohexane. The relative affinity of each model functionality was concentration dependent, yielding different relative affinity rankings among the functionalities at low and high concentrations.

The monolayer amounts achieved by each model functionality were obtained by applying the Langmuir model for adsorption in the form of

$$C/\sigma = C/\sigma_m + 1/b\sigma_m$$

where C, σ, σ_m, and b denote equilibrium concentration, amount adsorbed per unit weight of adsorbent, saturated monolayer amount, and a constant, respectively. Good conformity to the Langmuir model was obtained for each compound except pyrene. The monolayer amounts ranged from 1.3953 to 0.4444 mmol/g of silica, with phenol exhibiting the largest and pyrene, the smallest (Table 2). As the constant b is known to be related to the strength of the adsorptive forces (*7*), phenylsulfoxide, having a very high b value, should be the most strongly adsorbed functionality.

Competitive Adsorption

Competitive adsorption for the aggregate surface among asphalt functionalities is important because asphalt contains a multiplicity of compounds, each competing for the aggregate surface. Adsorption onto silica from bicomponent solutions was performed at a fixed initial solution concentration of 40 mmol, where monolayer coverage was achieved for all compounds. Both dry and moist (10 weight percent water) silica was used.

Six binary compound combinations with quinoline as reference were adsorbed onto dry silica (Table 3). Quinoline was selected as a reference because it showed a strong adsorption and an adsorption isotherm yielding a level plateau. For each combination, each component adsorption rate was rapid, with equilibrium being established within 5 min. The lesser adsorbed compound reached equilibrium more quickly than the more adsorbed. Only phenylsulfoxide showed a stronger competition for the silica surface than quinoline. Phenol and benzoic acid adsorbed nearly the same amount in the presence of quinoline; therefore, it was difficult to distinguish their competitive rankings. Benzophenone, benzylbenzoate, and pyrene showed large decreases in the amount adsorbed with quinoline present. The adsorption of benzylbenzoate was completely blocked, whereas pyrene was able to compete for sites in the presence of quinoline. Because of these factors, establishment of competitive ranking of benzylbenzoate and pyrene was difficult and required further experimentation.

The competitive edge of the different functionalities can be defined as

$$\text{Competitive Edge} = (1.00 - \text{Relative Reduction}) \times 100 \text{ percent}$$

where relative reduction is the percent decrease in the test compound divided by the percent decrease in the reference. The competitive edge for the different model functionalities relative to quinoline on dry silica given in Table 4 showed

TABLE 2 MONOLAYER AMOUNTS OF MODEL FUNCTIONALITIES ON SILICA

Model Compound	Correlation Coefficient (r)	Monolayer (mmol/g)	Constant, b (l/mmol)
Phenol	0.9994 (E)	1.3953	0.3608
Quinoline	0.9993 (E)	1.1983	0.6848
Phenylsulfoxide	0.9988 (C)	0.7369	2.7588
Benzoic Acid	0.9997 (E)	0.8890	0.6251
Benzophenone	0.9993 (E)	0.6092	0.2844
Benzylbenzoate	0.9995 (C)	0.5187	0.3554
Pyrene	0.9744 (E)	0.4444	0.0188

(E)entire isotherm used
(C)concave portion of isotherm used

TABLE 3 COMPETITIVE ADSORPTION OF BICOMPONENT SOLUTIONS ONTO DRY AND MOIST SILICA

Competitors on Dry Silica	Amount Adsorbed (mmol/g) Bicomponent (A)	Single Component (B)	Loss of Adsorption, %[a]
Quinoline	0.474	1.135	58.2
Phenylsulfoxide	0.611	0.970	37.0
Quinoline	0.797	1.130	29.5
Phenol	0.660	1.220	45.9
Quinoline	0.884	1.130	21.8
Benzoic Acid	0.656	0.840	21.9
Quinoline	0.991	1.130	12.3
Benzophenone	0.098	0.535	81.7
Quinoline	0.965	1.130	14.6
Benzylbenzoate	0.000	0.610	100.0
Quinoline	0.992	1.130	12.2
Pyrene	0.089	0.210	57.6
Phenylsulfoxide	0.723	0.955	24.3
Phenol	0.537	1.230	56.3
Phenylsulfoxide	0.826	0.935	11.7
Benzoic Acid	0.359	0.850	57.8
Benzylbenzoate	0.543	0.550	1.3
Pyrene	0.063	0.210	70.0

Competitors on Moist Silica	Amount Adsorbed (mmol/g) Moist Silica (A)	Dried Silica (B)	Loss of Adsorption, %[a]
Quinoline	0.283	0.474	40.3
Phenylsulfoxide	0.594	0.611	2.8
Quinoline	0.573	0.797	28.1
Phenol	0.614	0.660	7.0
Quinoline	0.670	0.884	24.2
Benzoic Acid	0.533	0.656	18.8

a, % = [(B-A)/B] x 100%

TABLE 4 COMPETITIVE EDGE OF DIFFERENT ASPHALT FUNCTIONALITIES IN RELATION TO A GIVEN REFERENCE ON DRY AND MOIST SILICA

	Competitive Edge (%) on Dry Silica		
Model Asphalt Functionalities	Relative to Quinoline	Relative to Phenylsulfoxide	Relative to Benzylbenzoate
Phenylsulfoxide	+36	0	
Quinoline	0		
Phenol	-56	-132	
Benzoic Acid	0	-394	
Benzophenone	-564		
Benzylbenzoate	-585		0
Pyrene	-372		-528

	Competitive Edge (%) on Moist Silica	
	Relative to Quinoline	Gain in Competitive Edge Compared to Dry Silica
Phenylsulfoxide	+93	57
Phenol	+75	131
Benzoic Acid	+22	22

that phenylsulfoxide had a positive competitive edge. Benzoic acid was not affected by the presence of quinoline; in contrast, phenol, pyrene, benzophenone, and benzylbenzoate did not successfully compete against quinoline.

Additional competitive adsorption experiments were performed to differentiate between the competitiveness of the two pairs: benzoic acid-phenol and benzylbenzoate-pyrene. Phenylsulfoxide served as reference for benzoic acid and phenol. Both benzoic acid and phenol were less competitive than phenylsulfoxide, with benzoic acid showing a smaller influence on phenylsulfoxide adsorption than did phenol, as well as a larger reduction from the single component affinity (Table 3). Therefore, phenol should be ranked as being more competitive than benzoic acid for the dry silica surface. Bicomponent adsorption experiments using the benzylbenzoate and pyrene system showed that the adsorption of pyrene was significantly affected by benzylbenzoate, but that of benzylbenzoate was unaffected by pyrene, making benzylbenzoate more competitive (Table 3).

The competitive affinity of the asphalt functionalities on dry silica can be ranked as phenylsulfoxide > quinoline > phenol > benzoic acid > benzophenone> benzylbenzoate > pyrene.

Competitive Adsorption Using Moist Silica

The sensitivity of the four most competitive functionalities to moisture on the silica surface was determined as shown in Table 3. The adsorbed water coverage of the silica surface was estimated to be 2.23 monolayers, indicating a multilayer. This calculation was based on the assumption that 1 water molecule interacts with 1 surface hydroxyl group and a silanol density of 5 $-OH/nm^2$ (*8,9*). Although the surface silanol groups were completely covered by water, the model compounds adsorbed significantly on the surface, with the water molecules acting as new adsorption sites (*10*). The adsorption rate of each compound was rapid, attaining equilibrium within a few minutes. Quinoline showed the greatest percent decrease in adsorption on moist silica compared with that on dry silica. When moisture sensitivity is defined as the decrease in adsorption from dry silica, the moisture sensitivity of the four compounds ranked as quinoline > benzoic acid > phenol > phenylsulfoxide.

On moist silica, the competitive edges of all three compounds relative to quinoline were positive and, thus, were increased compared with the dry silica case (Table 4). The gain in competitive edge ranged from 22 percent for benzoic acid to 131 percent for phenol. Thus, the oxygen-containing functionalities exhibited higher affinity than did the nitrogen base for the additional adsorption sites provided by the preadsorbed water.

Adsorption of AC-20 and Oxidized Asphalt

Adsorption onto Dry Silica

The adsorption of AC-20 and oxidized asphalts was performed in a continuous adsorption apparatus (*11*) where the initial

asphalt concentration was varied and the silica amount was held constant. Figure 2 shows the adsorption of AC-20, 32,000 poise asphalt, and 126,000 poise asphalt onto dry silica. For each oxidation level, the adsorption tended to follow a curve that formed a plateau at higher concentrations. The oxidized asphalts achieved less adsorption but yielded more level plateaus than AC-20.

The data obtained from AC-20 and oxidized asphalt adsorptions were fitted to both the Langmuir and Freundlich adsorption isotherms. The Langmuir model used was in the same form as stated earlier. The Freundlich equation was in the form

$$\ln \sigma = \ln K + (1/n)\ln C$$

where σ, C, K, and $1/n$ denote the amount adsorbed per unit weight of adsorbent, equilibrium concentration, and constants, respectively. The Langmuir model generally represents a homogeneous surface on which chemisorption and low-coverage physisorption occur and where monolayer coverage is probable, whereas the Freundlich equation generally describes a heterogeneous surface where physisorption occurs. The Langmuir model yielded a higher degree of linearity, with correlation coefficients ranging from 0.9856 to 0.9952, compared with 0.8649 to 0.9927 for the Freundlich model, with each individual comparison having a higher correlation coefficient for the Langmuir equation. According to the monolayer amounts obtained from the Langmuir equation (Table 5), the oxidized asphalts were less adsorbed on dry silica than

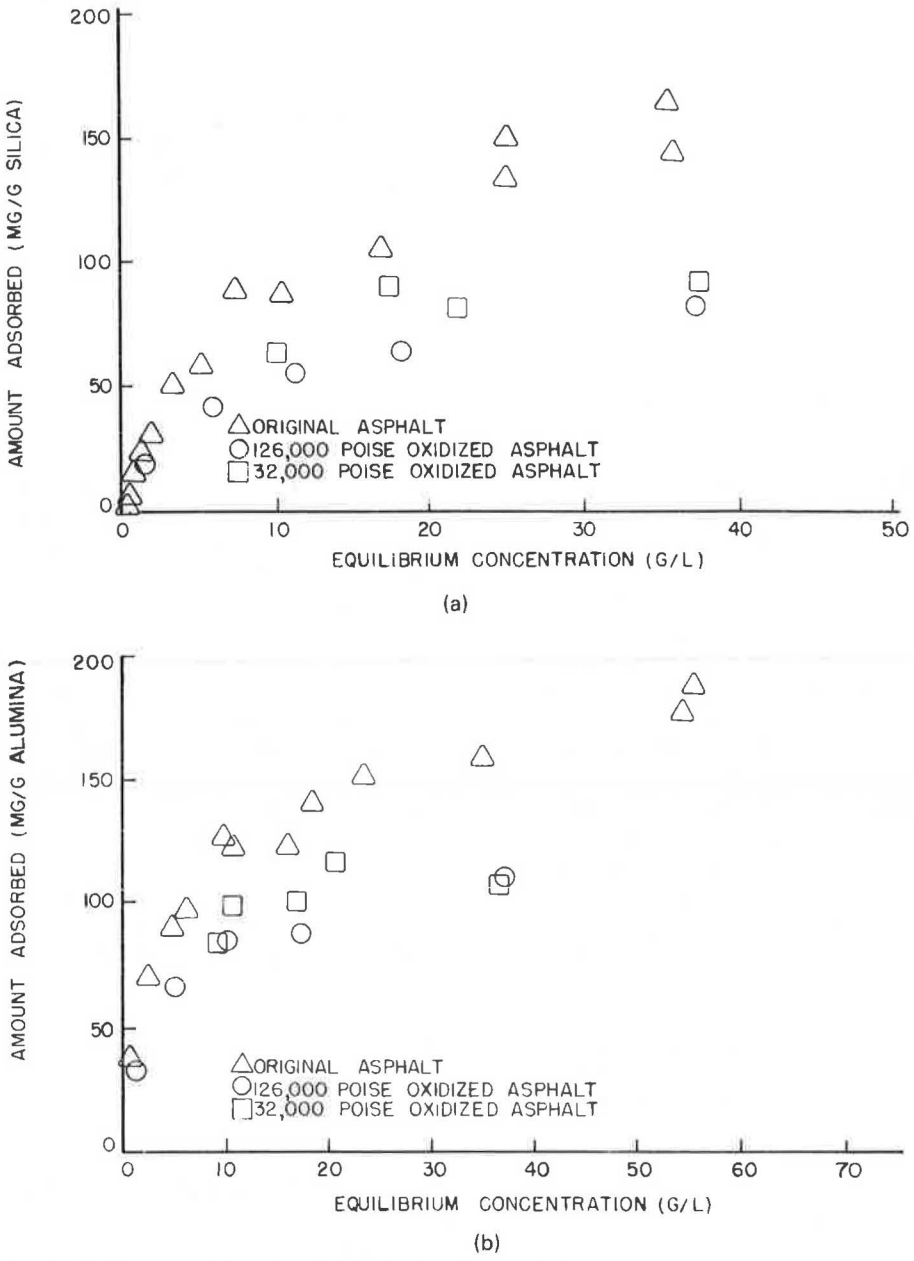

FIGURE 2 Adsorption of asphalt onto dry silica and dry alumina. (a) Adsorption of asphalt onto dry silica, (b) adsorption of asphalt onto dry alumina.

TABLE 5 MONOLAYER AMOUNTS OF AC-20 AND OXIDIZED ASPHALTS ADSORBED ONTO AGGREGATES

Asphalt Monolayer Amounts on a Weight Basis

Asphalt Viscosity, poise	Monolayer Amounts on Different Aggregates (mg/g)					
	Dry Silica	Moist Silica	Dry Alumina	Moist Alumina	Sandstone	Limestone
2,000	188	205	194	183	1.40	1.78
32,000	106		118			
126,000	93.5	93.8	119	118	1.25	1.72

Asphalt Monolayer Amounts on a Surface Area Basis

Asphalt Viscosity, poise	Monolayer Amounts on Different Aggregates (mg/m^2)					
	Dry Silica	Moist Silica	Dry Alumina	Moist Alumina	Sandstone	Limestone
2,000	0.638	0.697	0.538	0.508	2.06	2.77
32,000	0.359		0.327			
126,000	0.318	0.319	0.332	0.328	1.85	2.67

Asphaltenes Monolayer Coverage of the Real Aggregates

Asphalt Viscosity, poise	Monolayer Amounts: Weight Basis (mg/g)		Surface Area Basis (mg/m^2)	
	Sandstone	Limestone	Sandstone	Limestone
2,000	0.542	0.656	0.800	1.02
126,000	0.502	0.567	0.742	0.881

AC-20; the 32,000 poise asphalt was 43.7 percent less adsorbed, and the 126,000 poise asphalt was 50.1 percent less adsorbed.

Adsorption onto Moist Silica

AC-20 asphalt and 126,000 poise oxidized asphalt were also adsorbed onto silica that contained 5 weight percent water. The AC-20 adsorption behavior on moist silica was very similar to that on dry silica (Figure 3A), showing curves that appeared to form plateaus at high concentrations. The amount adsorbed on moist silica appeared to be higher than that on dry silica. The amount adsorbed was calculated on a dry aggregate basis, which means that the grams of asphalt adsorbed on moist silica were divided by the theoretical amount of dry silica used.

The adsorption data of moist silica fitted the Freundlich isotherm better than the Langmuir; however, the difference in the correlation coefficients was small (0.9954 for Freundlich versus 0.9677 for Langmuir). The AC-20 monolayer amount on moist silica was 9.4 percent higher than that on dry silica (Table 5).

The adsorption behavior of 126,000 poise oxidized asphalt onto moist and dry silica was similar, as shown in Figure 3B. The moist silica adsorption data fitted the Langmuir equation better than the Freundlich, with correlation coefficients of 0.9893 and 0.9551, respectively. The difference in monolayer amounts between the moist and dry silica obtained from the Langmuir correlation was only 0.32 percent. This small difference indicated that the adsorbed water on the silica surface had no effect on the monolayer amount of 126,000 poise oxidized asphalt adsorbed.

CAEM of Adsorbed Asphalt on Dry Silica

Previous CAEM studies performed by Rodriquez and coworkers (*12*) have shown that when carbonaceous deposits

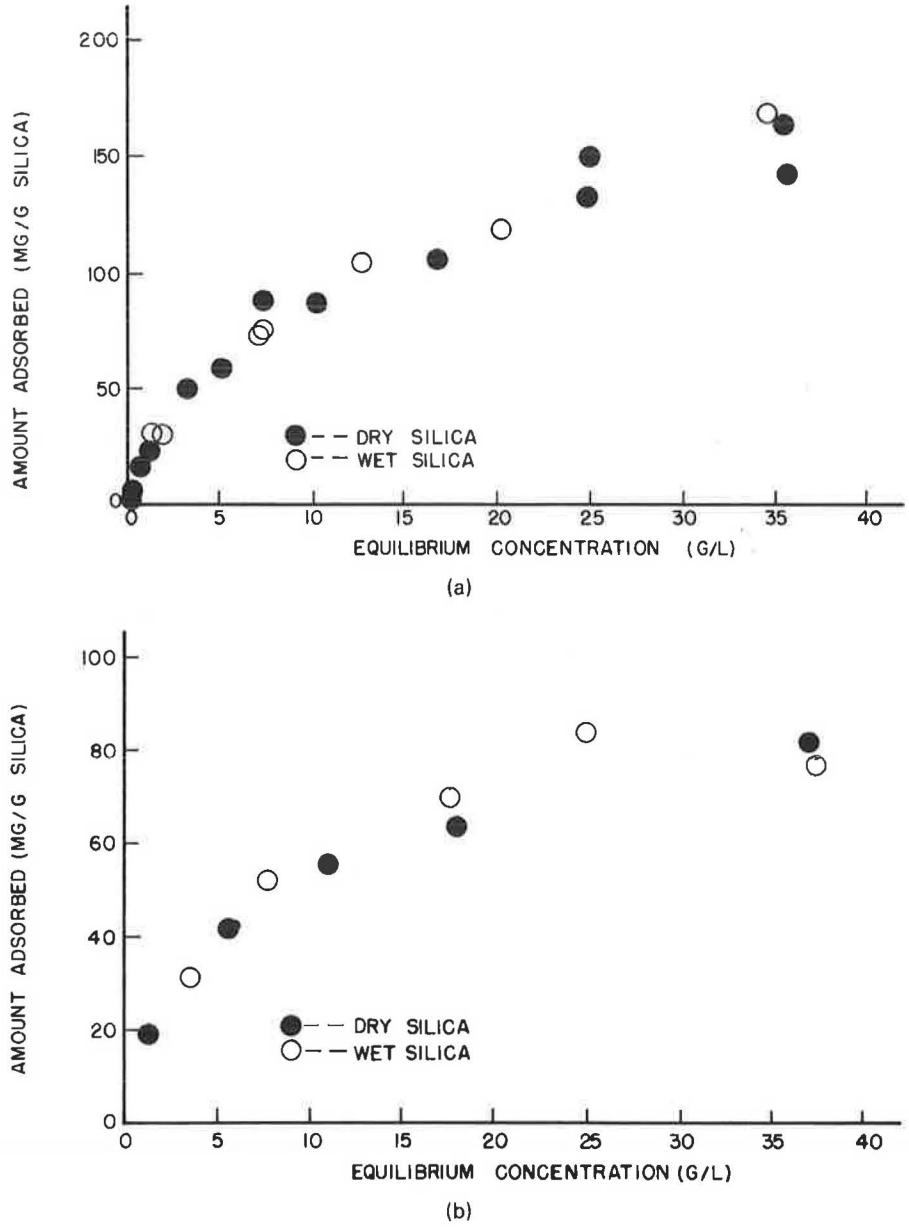

FIGURE 3 Adsorption of AC-20 and 126,000 poise asphalt onto dry and moist silica. (a) Adsorption of AC-20 asphalt, (b) adsorption of 126,000 poise oxidized asphalt.

were heated in 2 to 5 torr oxygen, the amorphous carbon was removed at temperatures between 450 to 650°C. Material that contained a significant amount of hydrogen was removed at the lower end of this temperature range. At 650°C, the inner core of filamentous carbon started to gasify and, upon a temperature increase to 750°C, the skin disappeared. Finally, at 850°C, any graphitic components present underwent oxidation.

Examination of the adsorbed asphalt on silica samples by CAEM at room temperature showed that individual sections of the samples were similar in appearance to the dry uncoated silica. The adsorbed asphalt samples exhibited an irregular "feathery" outline and were too dense to allow penetration by the electron beam. Hence, the observations were made at or near the edges of the material (Figure 4A). The adsorbed asphalt began to gasify between 425 and 460°C when the silica edges became lighter. At 475°C, the interior of the particle became lighter, indicating that the asphalt had been adsorbed into the silica pores. No further changes were observed with increased temperature.

As the adsorbed asphalt was removed, an accumulation of small particles, shown as the circled features in Figure 4B on the graphite support immediately adjacent to the silica fragments, was observed. The size and number of the particles increased with increased temperature. At 705°C, some of the particles started to catalytically oxidize the graphite support. Because this behavior was restricted to regions in the vicinity of the silica fragments with adsorbed asphalt and was not observed with the dry uncoated silica, it is most likely that the metal species originated from the adsorbed asphalt (*13*).

The observation that the adsorbed asphalt gasified in a uniform fashion at a relatively low temperature suggests that

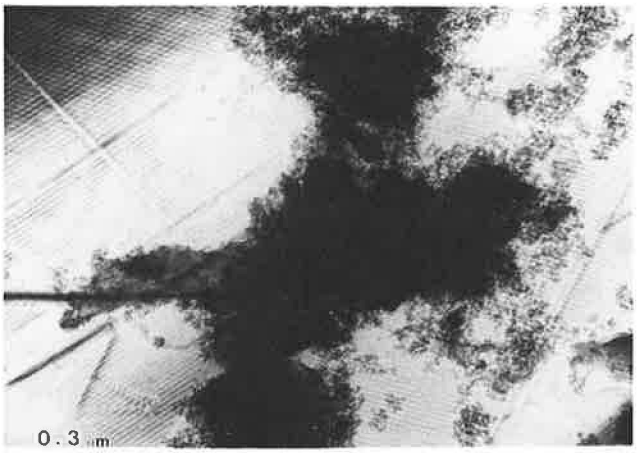

(a)

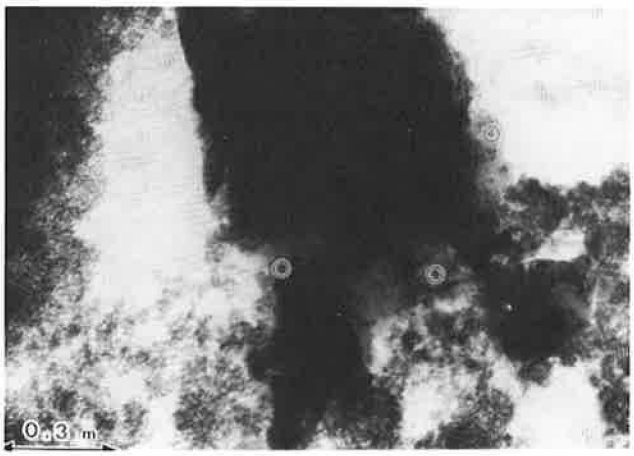

(b)

FIGURE 4 Transmission electron micrograph. (a) Asphalt adsorbed onto silica supported on graphite, (b) asphalt adsorbed onto silica with points corresponding to metallic impurities.

the adsorbed asphalt was amorphous and contained a significant amount of hydrogen. Even though metal was found in the deposit, no evidence was found for the formation of either filamentous or graphitic carbon on the surface of the silica.

Adsorption onto Dry Alumina

The adsorption of AC-20 and oxidized asphalts onto dry alumina given in Figure 2 showed two levels of adsorption: one for AC-20 and a lower level for the two oxidized asphalts. At higher concentrations, all of the isotherms began to form plateaus with the aggregate surface becoming saturated with adsorbed asphalt. Application of the Langmuir and Freundlich models showed that the Langmuir modeled the data better, yielding correlation coefficients of 0.9919 to 0.9960, compared with 0.7521 to 0.9866 for the Freundlich. Again, each individual comparison was better for the Langmuir model. The monolayer amounts given in Table 5 show that the 32,000 and 126,000 poise oxidized asphalts were ~39 percent less adsorbed than AC-20 whereas the difference between the two oxidized asphalts was only 1.3 percent. The amount adsorbed was affected by oxidation but not by the degree of oxidation.

Adsorption onto Moist Alumina

AC-20 appeared to adsorb less on moist alumina than on dry alumina, as shown in Figure 5A, an outcome that was opposite the moist silica results. The adsorption data for AC-20 using moist alumina fitted the Freundlich model better than the Langmuir model, although the difference in the correlation coefficients, 0.9898 compared with 0.9814, was small. The monolayer of AC-20 adsorbed on dry alumina was ~5.7 percent higher than that adsorbed onto moist alumina. Thus, the adsorbed surface water on alumina inhibited some of the AC-

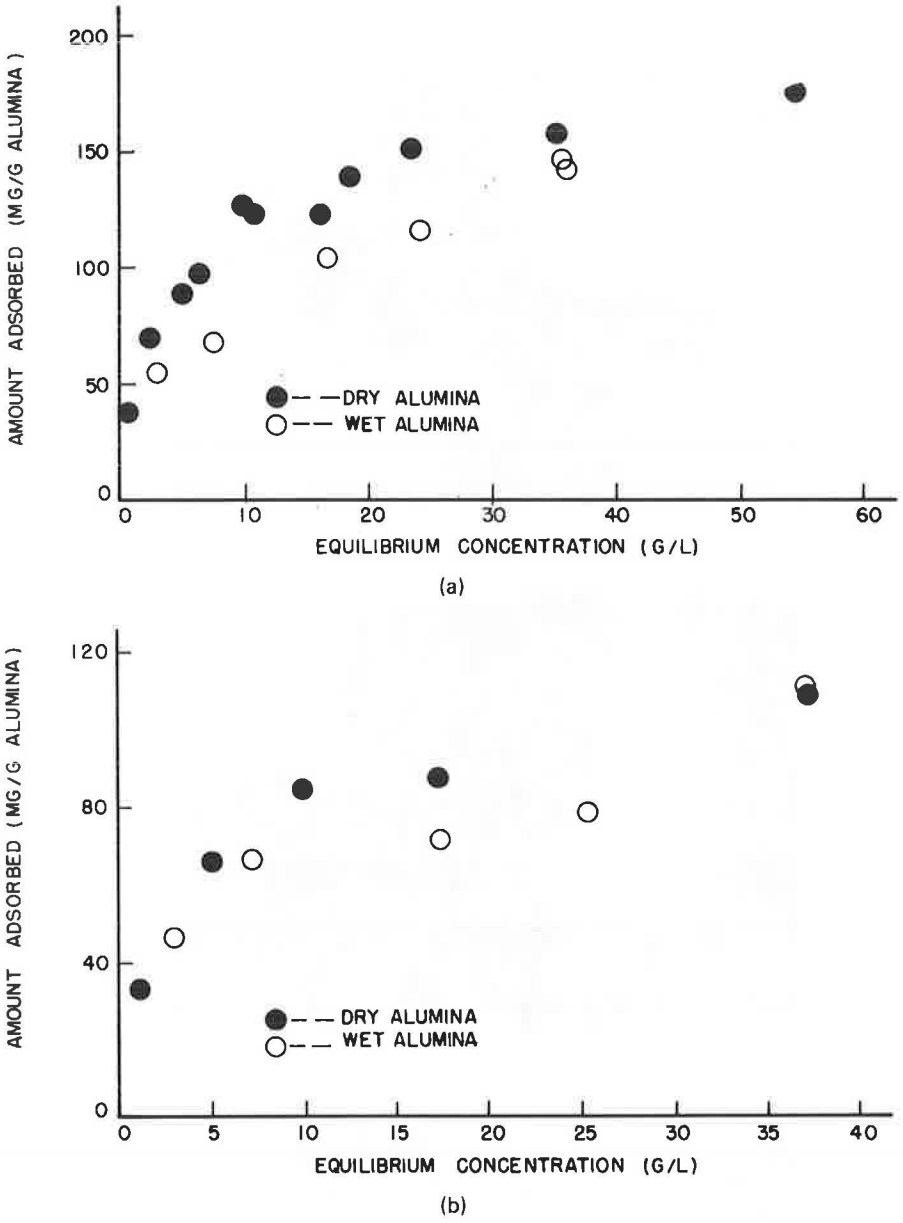

FIGURE 5 Adsorption of AC-20 and 126,000 poise asphalt on dry and moist alumina. (a) Adsorption of AC-20 asphalt, (b) adsorption of 126,000 poise oxidized asphalt.

20 from adsorbing, possibly through blocking or changing the acidity of some of the adsorption sites.

By contrast, the adsorption data for 126,000 poise asphalt on moist alumina (Figure 5B) fitted the Langmuir equation better than the Freundlich. Correlation coefficients for the models were 0.9525 and 0.9418, respectively. The monolayer amount (Table 5) for 126,000 poise asphalt on dry alumina was only 0.84 percent higher than that obtained with moist alumina.

Adsorption onto Sandstone

The adsorptive behavior of AC-20 and two oxidized asphalts on dry sandstone exhibited concentration dependence as presented in Figure 6. At low concentrations, the oxidized asphalts adsorbed more than AC-20, but at higher concentrations the reverse was true. The AC-20 isotherm reached an asymptote, whereas the oxidized isotherm showed a peak in the adsorption amount so that, at the highest concentrations, the amount of oxidized asphalt adsorbed decreased. This behavior may be due to the increased polarity of the oxidized asphalt compared with that of AC-20. Because an increase in polar group concentration increases the availability of hydrogen bonding groups, the oxidized asphalt tended to remain in solution at high concentrations rather than to adsorb to the aggregate because of a stronger association among the polar asphalt molecules (*14–16*).

The model functionality study showed that ketone groups were less adsorbed onto siliceous aggregate than carboxylic acids, sulfoxides, phenolics, and nitrogen bases. Because ketones are believed to be a major product of asphalt oxi-

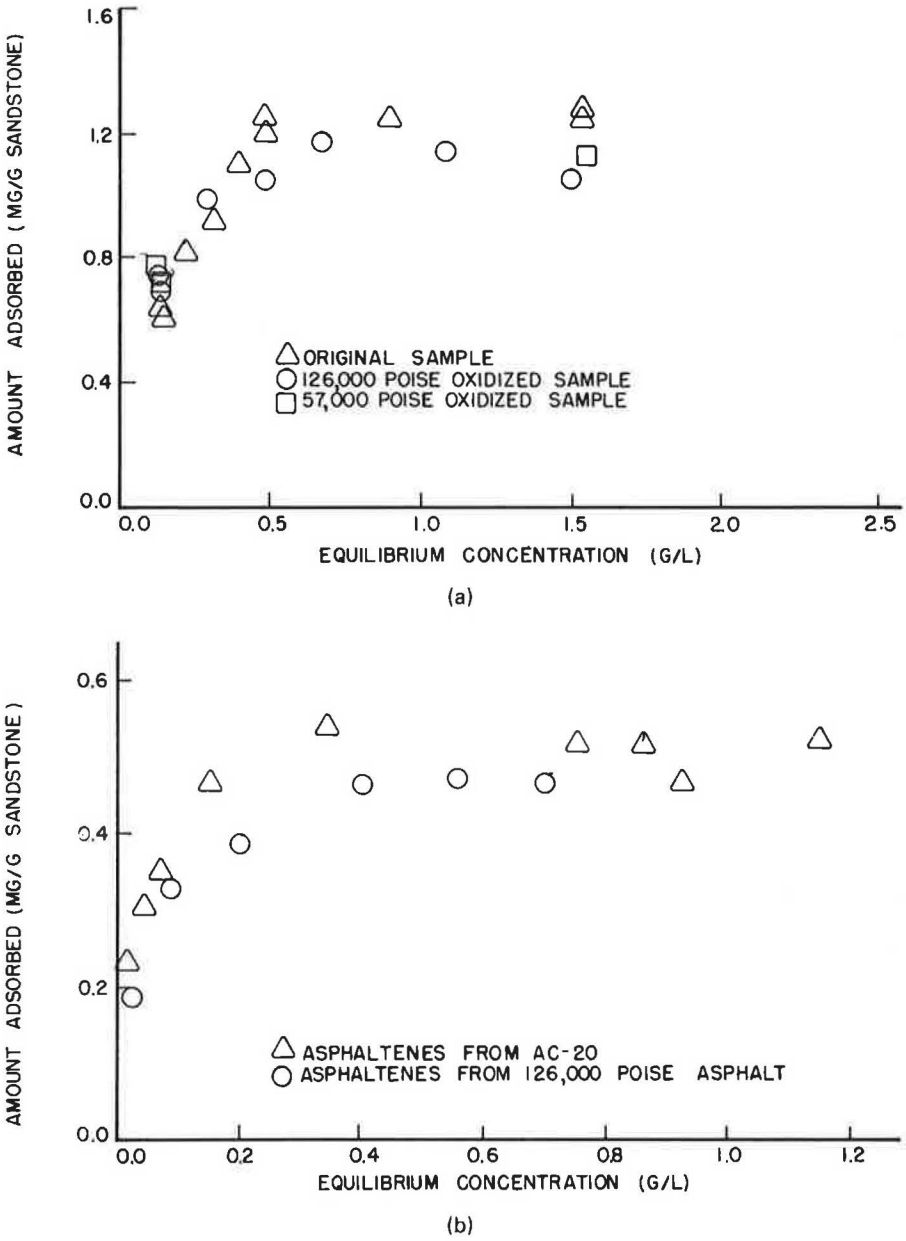

FIGURE 6 Adsorption of asphalt and asphaltenes onto sandstone. (a) Asphalt adsorption, (b) asphaltene adsorption.

dation (*3,17,18*), the chemical composition of the oxidized asphalt was changed compared with AC-20; hence, the total amount adsorbed should be less than AC-20. The concentration dependence observed in the adsorptive behavior of some model functionalities can be applied to that of asphalt on sandstone. Because the asphalt chemical composition changed with oxidation, the different chemical constituents present may have different relative affinities at high and low concentrations.

Infrared analyses of the oxidized asphalts produced for this study showed changes in their chemical composition as asphalt oxidation increased. Substantial increases in the ketone infrared absorbances were observed with increased asphalt viscosity (Figure 7A); changes in the sulfoxide absorbances were also observed (Figure 7B). Comparisons of the ketone and sulfoxide peak area ratios of the oxidized asphalts with those of AC-20 are given in Table 6. The ratios of the ketone peak areas increased as the oxidation increased, particularly for 32,000 and 57,000 poise asphalts. Similar increases were observed for asphaltenes. The sulfoxide absorbances showed different behavior. For the lesser oxidized asphalts of 7,000 and 32,000 poise, the sulfoxide peak area actually decreased. Asphaltenes showed lower sulfoxide peak areas only in the 7,000 poise asphaltenes compared with that of AC-20; all other oxidized asphaltenes contained more sulfoxides.

Asphaltene fractions from both AC-20 and 126,000 poise oxidized asphalt were adsorbed onto sandstone as shown in Figure 6B. AC-20 asphaltenes adsorbed more than the oxidized asphaltenes, giving a higher percent difference at low concentrations than at high concentrations.

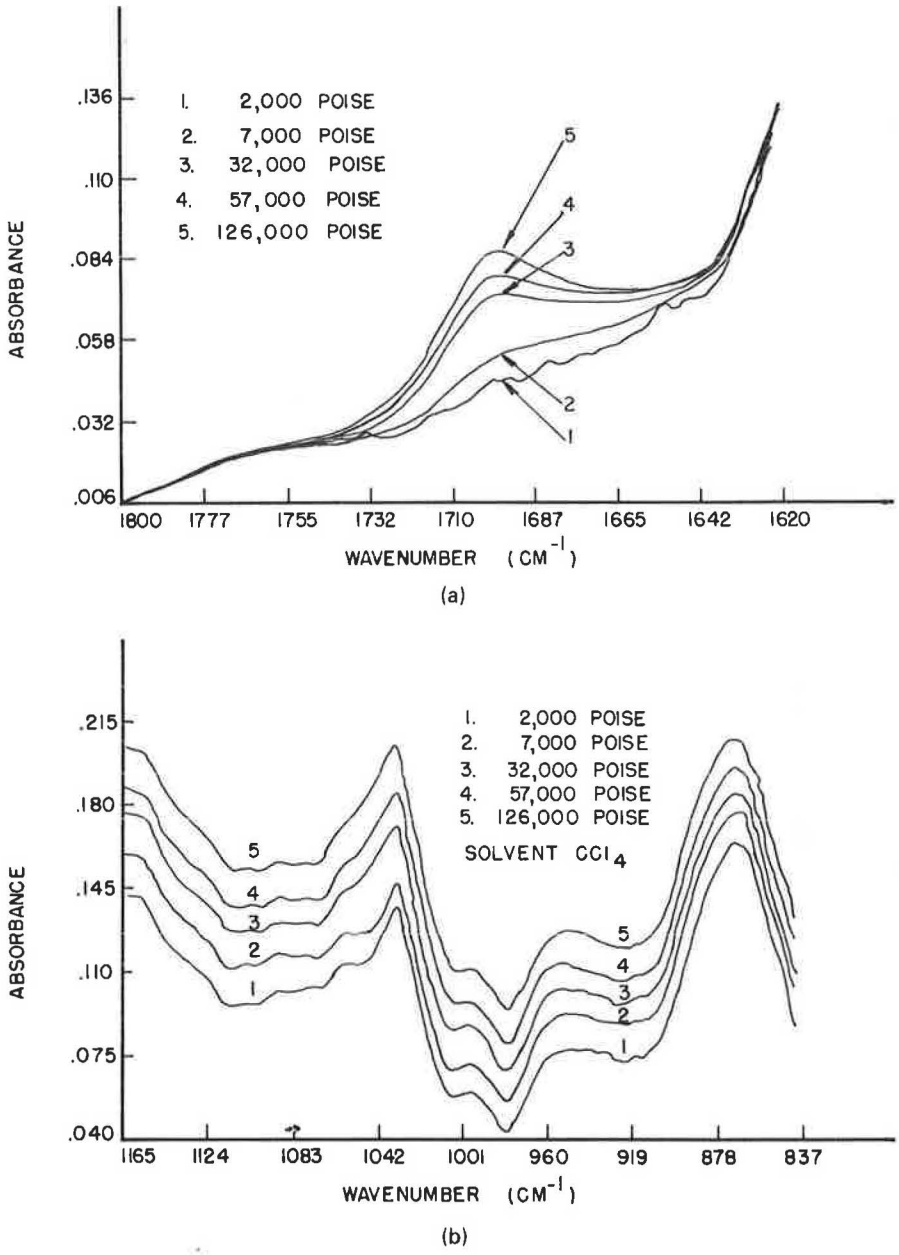

FIGURE 7 Infrared absorbances of AC-20 and oxidized asphalts. (a) Infrared ketone absorbances, (b) infrared sulfoxide absorbances.

Application of the Langmuir and Freundlich isotherms to both the asphalt and asphaltene adsorptions on sandstone showed that the Langmuir model provided a better fit for the data, yielding correlation coefficients ranging from 0.9972 to 0.9993 compared with 0.8721 to 0.9866 for the Freundlich. Monolayer amounts (Table 5) showed a 10.1 percent difference between AC-20 and oxidized asphalt and a 7.3 percent difference between AC-20 and oxidized asphaltenes.

Adsorption onto Limestone

The adsorptive behavior of AC-20 and oxidized asphalt onto limestone showed concentration dependence just as did their adsorption onto sandstone. At low concentrations, AC-20 adsorbed less than the oxidized asphalt but adsorbed more at higher concentrations. An asymptote was observed for AC-20 adsorption in Figure 8A and a peak with a maximum for the oxidized asphalt. The rationale given for the lowered adsorption of concentrated oxidized asphalt on sandstone can also be used for limestone. Adsorption of asphaltenes (Figure 8B) showed that the oxidized asphaltenes were more adsorbed than AC-20 asphaltenes at low concentrations; at high concentrations, the data were erratic.

The Langmuir model provided a better fit for both the asphalt and asphaltene data than did the Freundlich. The correlation coefficients for the Langmuir ranged from 0.9959 to 0.9991 and for the Freundlich, from 0.8635 to 0.9332. Because

TABLE 6 RATIOS OF KETONE AND SULFOXIDE PEAK AREAS IN CCl_4

Asphalt Viscosity, poise	Ketone Peak[a] Ratio Asphalts	Ketone Peak[a] Ratio Asphaltenes	Sulfoxide Peak[b] Ratio Asphalts	Sulfoxide Peak[b] Ratio Asphaltenes
2,000	0.0	0.0	1.0	1.0
7,000	0.1748	0.1649	0.7331	0.9055
32,000	0.6208	0.6543	0.9798	1.224
57,000	0.7606	0.7844	1.023	1.274
126,000	1.0	1.0	1.064	1.390

[a]The ketone region peak from AC-20 was numerically subtracted from the oxidized asphalts. The ketone peak areas were then ratioed to the 126,000 poise asphalt. The same procedure was used for the asphaltenes.

[b]All the asphalt sulfoxide peak areas were ratioed to the AC-20 peak. The same procedure was used for the asphaltenes.

the monolayer amounts obtained for AC-20 and oxidized asphalt were very similar (Table 5), no apparent difference in the adsorption of AC-20 and oxidized asphalt could be discerned. In contrast, a larger difference, 13.5 percent, was observed between AC-20 and oxidized asphaltenes on limestone, with the AC-20 asphaltenes having the larger monolayer amount.

SUMMARY

The adsorption of asphalt functionalities onto silica clearly demonstrates that adsorption behavior is dependent on a number of factors, including type of chemical entity, polarity of the functionality, competition among functionalities, concentration of the functionality, and dryness or moistness of the silica surface. The adsorption affinities among the seven functionalities differed according to their concentrations. Competition among pairs of functionalities gave this affinity ranking for dry silica: phenylsulfoxide > quinoline > phenol > benzoic acid > benzophenone > benzylbenzoate > pyrene. Quinoline showed the most moisture sensitivity and phenylsulfoxide, the least.

The aggregate ranking of adsorbed AC-20 and oxidized asphalt on dry aggregate was alumina > silica > limestone > sandstone. The oxidized asphalts were less adsorbed than AC-20 for each aggregate except for limestone, where no significant difference was observed. The effect of aggregate surface area on adsorption was determined by dividing the monolayer amounts by the aggregate surface area (Table 5). The dry aggregate ranking according to the largest amount of asphalt adsorbed per unit surface area was limestone > sandstone > silica > alumina. The 126,000 poise asphalt showed the same ranking except that alumina adsorbed more than silica. When compared on a surface area basis, sandstone and limestone adsorbed four to five times more than silica and alumina. The lower adsorption of the model aggregates may be due to hindered diffusion of the asphalt molecules or limited entrance to the pores due to pore mouth plugging.

Similar behavior was observed between AC-20 and oxidized asphalt on moist silica and moist alumina as on their dry counterparts. However, AC-20 interacted differently with the two moist surfaces: the moist silica yielded higher levels of AC-20 adsorption, but moist alumina yielded less. The adsorption of the 126,000 poise oxidized asphalt was equivalent regardless of the surface moisture of the two aggregates. These results along with the adsorption behavior on the dry aggregate indicated that the AC-20 contained more active adsorption moieties than the oxidized asphalts.

Although these results were obtained using only one parent asphalt, the trends observed may be relatable to pavement performance. To fully apply the results, however, these studies should be extended to a diverse group of asphalts from different suppliers and crude sources. In addition, the inclusion of a wider variety of real and model aggregates would provide more information for predicting interactions between asphalts oxidized to different degrees and aggregates of different chemical compositions.

ACKNOWLEDGMENTS

The authors gratefully acknowledge Hunt Oil for provision of asphalt samples. The CAEM analyses provided by Terry Baker and Nelly Rodriquez of the Chemical Engineering Department, Auburn University, are gratefully acknowledged and appreciated. Thanks also go to Burton Davis of the Kentucky Center for Applied Energy Research for the oxygen analysis. The authors also gratefully acknowledge the Auburn University Highway Research Center and the National Center for Asphalt Technology for support of this work.

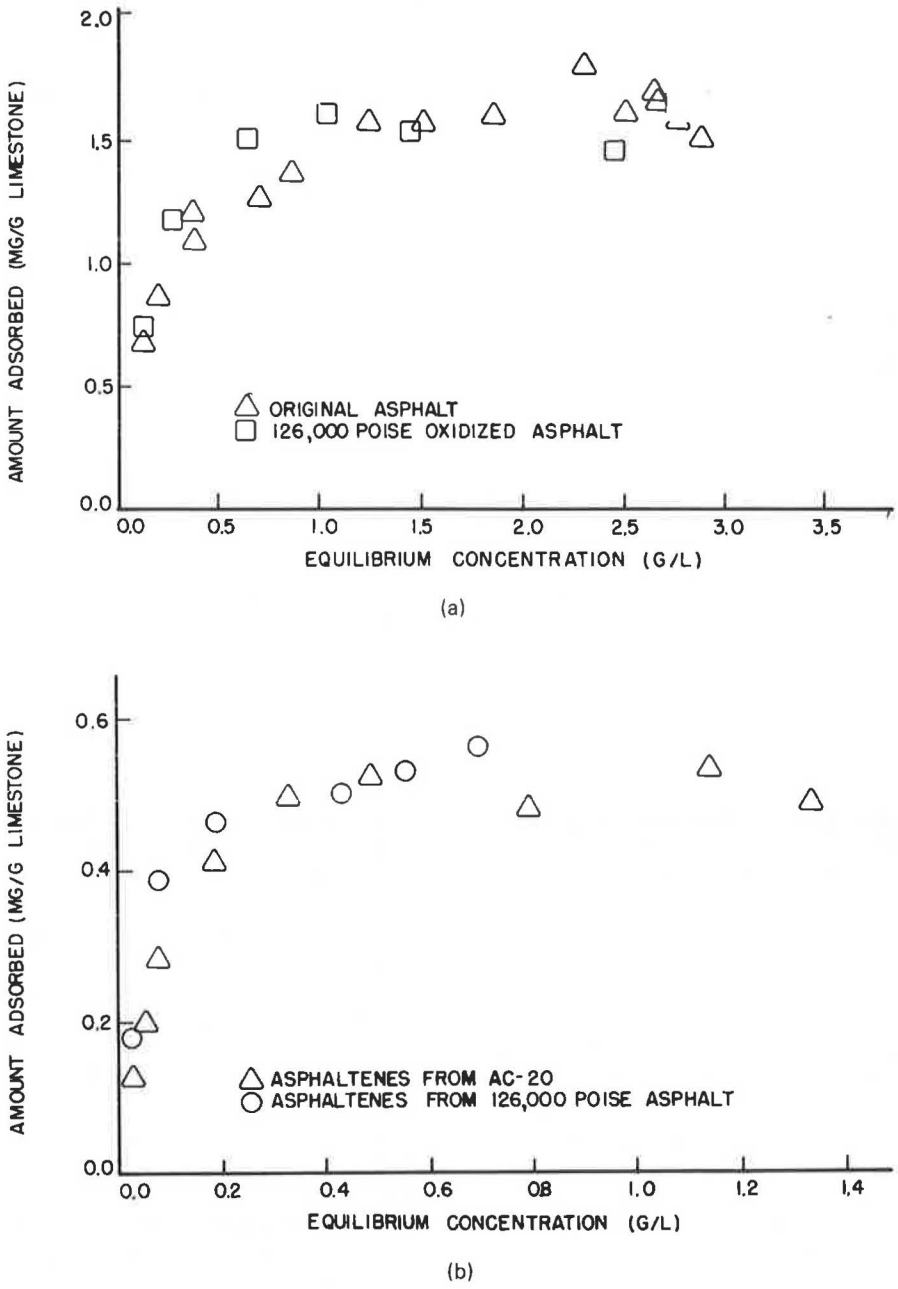

FIGURE 8 Adsorption of asphalt and asphaltenes onto limestone. (a) Adsorption of asphalt, (b) asphaltene adsorption.

REFERENCES

1. H. Plancher, S. M. Dorrence, and J. C. Petersen. Identification of Chemical Types in Asphalts Strongly Adsorbed at the Asphalt-Aggregate Interface and Their Relative Displacement by Water. *Proc., Association of Asphalt Paving Technologists*, Vol. 46, 1977, pp. 151–175.
2. J. C. Petersen. Quantitative Functional Group Analysis of Asphalt Using Differential Infrared Spectrometry and Selective Chemical Reactions—Theory and Application. In *Transportation Research Record 1096*, TRB, National Research Council, Washington, D.C., 1987, pp. 1–11.
3. J. C. Petersen, F. A. Barbour, and S. M. Dorrence. Identification of Dicarboxylic Anhydrides in Oxidized Asphalts. *Analytical Chemistry*, Vol. 47, 1975, pp. 107–111.
4. J. C. Petersen and H. Plancher. Quantitative Determination of Carboxylic Acids and Their Salts and Anhydrides in Asphalts by Selective Chemical Reactions and Differential Infrared Spectrometry. *Analytical Chemistry*, Vol. 53, 1981, pp. 786–789.
5. J. C. Petersen. Quantitative Method Using Differential Infrared Spectrometry for the Determination of Compound Types Absorbing in the Carboxyl Region in Asphalts. *Analytical Chemistry*, Vol. 47, 1975, pp. 112–117.
6. R. T. K. Baker. In situ Electron Microscopy Studies of Catalyst

Particle Behavior. *Catalysis Reviews: Science and Engineering*, Vol. 19, No. 2, 1979, pp. 161–209.
7. G. D. Parfitt and C. H. Rochester. *Adsorption from Solution at the Solid/Liquid Interface*. Academic Press, New York, 1983, chap. 1.
8. D. E. Yates and T. W. Healy. The Structure of the Silica/Electrolyte Interface. *Journal of Colloid and Interface Science*, Vol. 55, 1976, pp. 9–19.
9. J. F. Danielli, M. D. Rosenberg, and D. A. Cadenhead, eds. *Progress in Surface and Membrane Science*. Academic Press, New York, Vol. 5, 1972, pp. 96–113.
10. K. Tanabe. *Solid Acids and Bases*. Kodansha, Tokyo, 1970, Chap. 2.
11. J. Saint-Just. Catalyst Characterization by Adsorption of Petroleum Asphaltenes in Solution. *Industrial and Engineering Chemistry: Product Research and Development*, Vol. 19, 1980, pp. 71–75.
12. N. M. Rodriquez, H. Marsh, E. A. Heintz, R. D. Sherwood, and R. T. K. Baker. Oxidation Studies of Various Petroleum Cokes. *Carbon*, Vol. 25, 1987, pp. 629–635.
13. R. T. K. Baker and R. D. Sherwood. Catalytic Gasification of Graphite by Nickel in Various Gaseous Environments. *Journal of Catalysis*, Vol. 70, 1981, pp. 198–214.
14. E. K. Ensley. Multilayer Adsorption with Molecular Orientation of Asphalt on Mineral Aggregate and Other Substrate. *Journal of Applied Chemistry and Biotechnology*, Vol. 25, 1975, pp. 671–682.
15. D. M. Clementz. Interaction of Petroleum Heavy Ends with Montmorillonite. *Clays and Clay Minerals*, Vol. 24, 1976, pp. 312–319.
16. R. V. Barbour and J. C. Petersen. Molecular Interactions of Asphalt: An Infrared Study of the Hydrogen-Bonding Basicity of Asphalt. *Analytical Chemistry*, Vol. 46, 1974, pp. 273–277.
17. J. C. Petersen. Chemical Composition of Asphalt as Related to Asphalt Durability—State of the Art. In *Transportation Research Record 999*, TRB, National Research Council, Washington, D.C., 1985, 13–30.
18. S. M. Dorrence, F. A. Barbour, and J. C. Petersen. Direct Evidence of Ketones in Oxidized Asphalts. *Analytical Chemistry*, Vol. 46, 1974, pp. 2242–2244.

Publication of this paper sponsored by Committee on Characteristics of Bituminous Materials.